



Contents lists available at ScienceDirect

Journal of Cardiovascular Computed Tomography

journal homepage: www.JournalofCardiovascularCT.com

Research paper

Computed tomography anatomic predictors of outcomes in patients undergoing tricuspid transcatheter edge-to-edge repair

Joanna Bartkowiak^{a,b}, Hari Vivekanantham^{c,d,e}, Mohammad Kassar^e, Chrisoula Dernektsi^e, Vratika Agarwal^a, Mark Lebehn^a, Stephan Windecker^e, Nicolas Brugger^e, Rebecca T. Hahn^{a,1}, Fabien Praz^{e,*}

^a Department of Medicine, The NewYork-Presbyterian/Columbia University Irving Medical Center, New York, NY, USA

^b Graduate School for Health Sciences, University of Bern, Bern, Switzerland

^c Department of Cardiology, University and Hospital of Fribourg, Fribourg, Switzerland

^d Arrhythmia Services, Division of Cardiology, Department of Medicine, McMaster University, Hamilton, Ontario, Canada

^e Department of Cardiology, University of Bern, Inselspital, Bern, Switzerland

A B S T R A C T

Aim: To identify anatomical computed tomography (CT) predictors of procedural and clinical outcomes in patients undergoing tricuspid transcatheter edge-to-edge repair (T-TEER).

Methods and results: Consecutive patients undergoing T-TEER between March 2018 to December 2022 who had cardiac CT prior to the procedure were included. CT scans were automatically analyzed using a dedicated software that employs deep learning techniques to provide precise anatomical measurements and volumetric calculations. Technical success was defined as successful placement of at least one implant in the planned anatomic location without single leaflet device attachment. Procedural success was defined as tricuspid regurgitation reduction to moderate or less. Procedural complexity was assessed by measuring the fluoroscopy time. The clinical endpoint was a composite of death, heart failure hospitalization, or tricuspid re-intervention throughout two years. A total of 33 patients (63.6% male) were included. Procedural success was achieved in 22 patients (66.7%). Shorter end-systolic (ES) height between the inferior vena cava (IVC) and tricuspid annulus (TA) ($r = -0.398$, $p = 0.044$) and longer ES RV length ($r = 0.551$, $p = 0.006$) correlated with higher procedural complexity. ES RV length was independently associated with lower technical (adjusted Odds ratio [OR] 0.812 [95% CI 0.665–0.991], $p = 0.040$) and procedural success (adjusted OR 0.766, CI [0.591–0.992], $p = 0.043$). Patients with ES right ventricular (RV) length of >77.4 mm had a four-fold increased risk of experiencing the composite clinical endpoint compared to patients with ES RV length ≤ 77.4 mm (HR = 3.964 [95% CI, 1.018–15.434]; $p = 0.034$).

Conclusion: CT-derived RV length and IVC-to-TA height may be helpful to identify patients at increased risk for procedural complexity and adverse outcomes when undergoing T-TEER. CT provides valuable information for preprocedural decision-making and device selection.

1. Background

Tricuspid transcatheter edge-to-edge repair (T-TEER) is a minimally invasive procedure with a class IIb indication (level of evidence C) in the 2021 ESC/EACTS valvular heart disease guidelines for the treatment of patients with secondary tricuspid regurgitation (TR) at high surgical risk. Several studies attempted to define the anatomical characteristics predicting optimal results after T-TEER by the analysis of preprocedural echocardiographic images and associated smaller coaptation gap, antero-septal jet localization, and three-leaflet morphology with procedural success.^{1–3} However, conflicting data persist regarding the impact of other

parameters, including baseline effective regurgitant orifice area, tenting area, tenting height, right ventricular (RV) and tricuspid annulus (TA) diameter.^{1,2,4} The evaluation of these echocardiographic parameters can pose challenges and exhibit inherent variability, contingent upon the expertise and methodology of both image acquisition and quantitation.

The use of computed tomography (CT) to determine patient eligibility for T-TEER is not mandatory. However, CT is often performed in patients with TR to evaluate the feasibility of alternative transcatheter therapies, including annular repair devices, as well as orthotopic and heterotopic replacement devices. The utilization of CT offers several advantages, such as superior signal to noise ratio, and the ability to assess

Abbreviations: A-STR/V-STR, Atrial/Ventricular Secondary Tricuspid Regurgitation; CT, Computed Tomography; ED, End-Diastolic; ES, End-Systolic; IVC, Inferior Vena Cava; RA, Right Atrium; RV, Right Ventricle; TA, Tricuspid Annulus; T-TEER, Tricuspid Transcatheter Edge-to-Edge Repair; TR, Tricuspid Regurgitation.

* Corresponding author. Department of Cardiology, University of Bern, Inselspital, Bern, Switzerland.

E-mail address: fabien.praz@insel.ch (F. Praz).

¹ Dr. Praz and Dr. Hahn contributed equally to this publication and are joint last authors.

<https://doi.org/10.1016/j.jcct.2024.02.001>

Received 3 October 2023; Received in revised form 9 January 2024; Accepted 8 February 2024

Available online xxxx

1934-5925/© 2024 The Authors. Published by Elsevier Inc. on behalf of Society of Cardiovascular Computed Tomography. This is an open access article under the CC BY-NC-ND license (<http://creativecommons.org/licenses/by-nc-nd/4.0/>).

extracardiac structures and offset of the inferior vena cava (IVC) within the RA. Moreover, CT facilitates automated volumetric calculations using specialized software, thereby ensuring the accuracy, reliability, and reproducibility of the obtained measurements.^{5,6}

CT-derived predictors of procedural success in patients undergoing T-TEER have not been defined so far. The objective of the present study was to determine the CT-derived anatomical characteristics that impact procedural and clinical outcomes, as well as those associated with increased procedural complexity.

2. Methods

2.1. Study population

Consecutive patients undergoing T-TEER at the Cardiovascular Center, Bern University Hospital, Bern, Switzerland between March 2018 and December 2022 who had CT scans available as part of their eligibility screening for tricuspid valve interventions were retrospectively included in this observational study. All included patients were deemed inoperable by a multidisciplinary Heart Team.

3. CT protocol

Patients underwent electrocardiogram-gated CT following a dedicated tricuspid protocol. Intravenous injection of nonionic contrast agent (370 mg/ml – Iopromid) was performed using a triphase protocol as follows: 60%/40% contrast/saline mixture at a rate of 4 ml/s, followed by 25%/75% contrast saline mixture at a rate of 4 ml/s, and finally 20 ml of normal saline at 4 ml/s (total contrast volume = 61 ml). Tube current and potential were determined by the physician conducting the scan or by software automation according to the patient's weight and size. The 3D data set from the contrast-enhanced scan was reconstructed at 5% increments throughout the cardiac cycle. Images were reconstructed with a slice thickness of 0.5 mm.

3.1. Computed tomography analysis

For a comprehensive analysis of the CT datasets, we utilized Heart.ai's (LARALAB GmbH, Munich, Germany) software, applying advanced deep

learning techniques. Instead of solely relying on radio density thresholding to define borders, it utilizes algorithms developed through extensive training on a diverse array of CT scans. These algorithms have been validated and proven effective by clinical experts, ensuring an accurate delineation of borders. The software allows for 4D visualization of the heart's structural dynamics over the cardiac cycle (Fig. 1A). Characteristic heart planes for multiplanar views are calculated based on the 3D models (Fig. 1B), and custom algorithms are used to automatically derive a wide range of measurements, including TA area, TA perimeter, TA diameters (Fig. 1C), RA and RV height, RV length (dimension from middle of TA to RV apex) (Fig. 1D–F), IVC area, IVC perimeter and IVC diameters, as well as distance between middle of IVC and TA. The IVC and TA relationship is further defined by the anteroposterior (anteroposterior IVC-to-TA), septolateral (IVC-to-TA septo-lateral offset), and perpendicular (IVC-to-TA height) distances (Fig. 2).

The end-systolic (ES) and end-diastolic (ED) volumes of cardiac chambers were determined based on the highest and lowest calculated volumes observed during the cardiac cycle. For all other parameters, ES was defined as the 35–40% phase of the cardiac cycle, while ED was defined as the 95–0% phase. An experienced member of the research team (J.B.) visually confirmed all automatic measurements. TA and IVC areas, perimeters and diameters were manually corrected if needed, prior to inclusion into the analysis. Ventricular and atrial volumes and dimensions, as well as IVC-to-TA distances were analyzed automatically without manual correction. In patients without significant regurgitation of other valves, stroke volume, TR volume and TR fraction were calculated. Additionally, tenting height, tenting area, basal and mid-ventricular RV dimensions and anatomical regurgitant orifice area (the level of narrowest portion of regurgitant orifice) were manually measured in ES in four chambers view (Supplemental Figure 1). The supplemental material provides an additional information on automated CT algorithms, the formulas used for calculation of stroke volume, TR volume and TR fraction, as well as RV sphericity index.

3.2. Echocardiographic analysis

Baseline echocardiographic data were assessed in accordance with the European and American Echocardiography Guidelines.^{7,8} Effective regurgitant orifice area was quantified using the proximal isovelocity

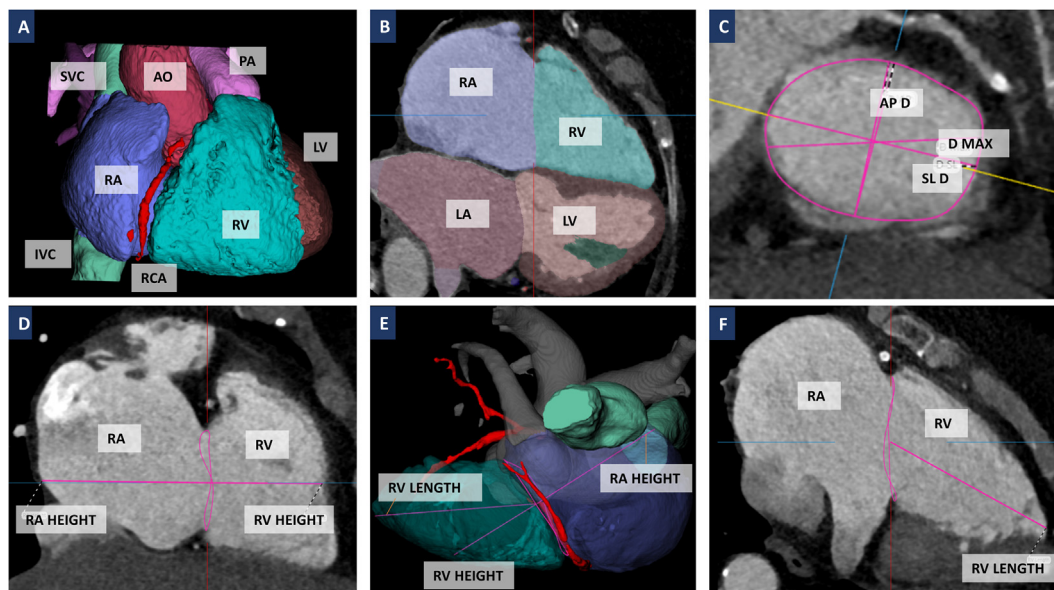


Fig. 1. Three dimensional (1A, 1E) and two dimensional (1B-1D, 1F) CT reconstructions with fully automated segmentation of all cardiac chambers and adjacent vessels. The study specific protocol included automated measurement of various parameters across multiple phases, including atrial and ventricular volumes and areas (1A-1B), TA dimensions (1C), as well as RA and RV heights (1D-1E) and RV length (1E-1F). Ao = Aorta, AP = Anteroposterior, D = Diameter, LA = Left Atrium, LV = Left Ventricle, PA = Pulmonary Artery, RCA = Right Coronary Artery, SVC = Superior Vena Cava.

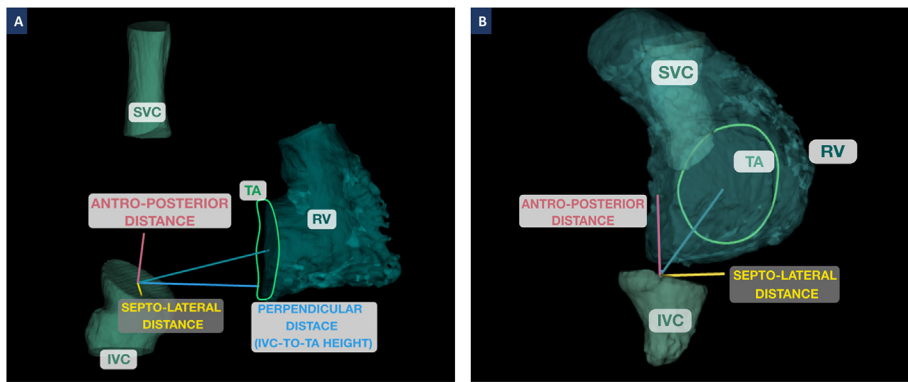


Fig. 2. Three-dimensional reconstruction of IVC, superior vena cava (SVC), and RV. The reconstruction process was fully automated, and included the measurement of the distances between the center of the IVC and the center of the TA (pink line). This distance was subsequently decomposed into three components, namely anteroposterior, septolateral, and perpendicular (IVC-to-TA height) distance. (For interpretation of the references to colour in this figure legend, the reader is referred to the Web version of this article.)

surface area measurement without corrections for flow or tenting angle. The severity of TR was assessed using a five grade severity scale integrating multiple quantitative and semiquantitative methods.^{8,9} Tenting height, tenting area and coaptation gap were measured in ES in apical four chamber view.¹⁰

3.3. Procedural outcomes

Procedural data was collected by retrospective analysis of patients' records. Technical success was defined as a successful implantation of at least one device and no single leaflet device attachment. Procedural success was defined as TR reduction to moderate (2+) or less degree at the end of the intervention. Procedural complexity was assessed by evaluation of fluoroscopy time of the whole procedure and fluoroscopy time needed to implant one device. Patients with concomitant mitral procedure were excluded from the analysis correlating procedural times with anatomical parameters.

3.4. Clinical outcomes

Clinical data was collected retrospectively from patients' records at one-month and yearly after the index procedure. The primary clinical endpoint was a composite of mortality, heart failure hospitalization, and tricuspid re-intervention up to 2 years following the procedure.

3.5. Statistical analysis

Differences in continuous variables between unpaired data were compared with unpaired T-Test or Mann Whitney test depending on normality. Unpaired nominal data were compared using Pearson Chi2 test and paired nominal data with McNemar test.

To determine intraobserver and interobserver reproducibility of manual CT and echocardiographic measurements, 8 patients were randomly selected and analyzed by the same operator (J.B. and M.K.) after at least two weeks and by a second blinded one (J.B. for echocardiographic analysis and C.D. for CT analysis), and then compared using intraclass correlation coefficient. The automated two-dimensional measurements were compared to manual measurements performed in the commercially accessible 3Mensio software (3Mensio Medical Imaging, Bilthoven, Netherlands) using Bland-Altman analysis to assess mean bias and 95% limits of agreement.

Correlations between continuous variables were explored with the Pearson correlation coefficient. Univariate logistic regression analysis was performed on all automated CT-derived parameters and possible echocardiographic predictors of procedural success (effective regurgitant orifice area, non-central, non-anteroseptal jet localization, tenting height, tenting area) to identify determinants of procedural and technical success. Cox regression analysis was performed on baseline variables that significantly varied between the groups stratified by primary outcome (Table 1) and by other predictors of poor clinical outcome in patients undergoing

transcatheter valve intervention and included: age, albumin, TAPSE/SPAP, renal disease, RV length, TAPSE, RV EF and PAPI (sPAP-diastolic PAP)/right atrial pressure). Selected covariates with a P-value of <0.05 at the univariate stage were included into multivariate models. If highly correlated variables were substantially associated with the outcomes of interest, the variable that best improved the predictive performance was included. Log rank test and Kaplan-Mayer estimates were created to assess the time to composite endpoint. A two-sided P value of <0.05 was considered to indicate statistical significance. All analyses were conducted with IBM SPSS Statistics V.18 (IBM Corporation, Armonk, NY, USA).

4. Results

4.1. Baseline characteristics

Among sixty patients who underwent T-TEER between 18.06.2018 and 19.12.2022, 33 had a CT scan available for analysis. Compared to the excluded patients (n = 27) undergoing T-TEER during the same period, renal disease and hypertension were more frequent in the excluded cohort (74% (20/27) vs. 45% (15/33), p = 0.025 and 96% (26/27) vs. 79% (26/33), p = 0.047, respectively). There were no significant differences observed in other clinical, echocardiographic, or hemodynamic parameters between the two groups. The median age of the study cohort was 79.9 ± 7.2 years. Twenty (60.6%) patients reported heart failure NYHA class III or IV. The median TRI-SCORE¹¹ was 5 [IQR 3.5–6.0] points. Moderate, severe, massive and torrential¹² TR was found in 1 (3%), 9 (27.3%), 13 (39.4%), 10 (30.3%) patients, respectively. TR etiology was primary in 12.1% (n = 4), A-STR in 39.4% (n = 13), and V-STR in 48.5% (n = 16) of the patients. The mean baseline effective regurgitant orifice area was 67.3 mm² ± 2.8 mm². The baseline characteristics of the study population are presented in Table 1.

4.2. Baseline CT derived parameters

All 49 CT-derived parameters, stratified by baseline TR, are listed in Supplemental Table 1. Volumes were calculated for all 33 patients. Two-dimensional ED dimensions were available in 31 and ES dimensions in 29 patients. The mean CT-derived TR volume and TR regurgitant fraction was 45.6 ml and 38.6% in patients with moderate/severe TR, 55.6 ml and 46.8% in patients with massive TR and 77.8 ml and 64.4% in patients with torrential TR respectively.

4.3. Automated versus manual CT-derived analysis

Supplemental Table 2 illustrates the agreement between automated and manual measurements. Notably, among the parameters examined, only the dimensions of the IVC displayed significant bias. This discrepancy may arise from the absence of standardized protocols for IVC measurements, often resulting in an unclear distinction between the IVC and RA. In contrast, other parameters exhibited a robust level of agreement.

Table 1

Baseline Characteristics Compared between the Patients Who Met the Combined Endpoint and those who did not.

	All patients	No event n = 19	Death, HF hospitalization or tricuspid re-intervention n = 14	P value
Age, y	79,9 (7,2)	82,3 (4,9)	76,7 (8,7)	0,026
Male	21 (63,6)	10 (52,6)	11 (78,6)	0,126
TRI-SCORE	5 [3,5–6,0]	5 [3,0–6,0]	5 [3,5–6,25]	0,724
CAD	14 (42,4)	7 (36,8)	7 (50)	0,497
Previous MI	9 (27,3)	4 (21,1)	5 (35,7)	0,317
AF	30 (90,9)	18 (94,7)	12 (85,7)	0,373
Pneumopathy	10 (30,3)	5 (25,3)	5 (35,7)	0,561
Hypertension	26 (78,8)	16 (84,2)	10 (71,4)	0,375
Dialysis	1 (3,0)	0 (0)	1 (7,1)	0,237
Liver disease	3 (9,1)	1 (5,3)	2 (14,3)	0,373
Renal disease	15 (45,5)	7 (36,8)	8 (57,1)	0,247
Pulmonary Hypertension	8 (24,2)	4 (21,1)	4 (28,6)	0,695
sPAP	40,1 (11,7)	39,5 (11,4)	40,8 (12,5)	0,876
mPCWP	18,4 (6,9)	20,2 (7,5)	16,7 (6,1)	0,777
RV lead	8 (24,2)	4 (21,1)	4 (28,6)	0,618
Previous cardiac surgery	8 (24,2)	5 (25,3)	3 (21,4)	0,802
Tricuspid	2 (6,1)	1 (5,3)	1 (7,1)	
Other valves	4 (12,1)	2 (10,5)	2 (14,3)	
CABG	1 (3,0)	1 (5,3)	0 (0)	
Other	1 (3,0)	1 (5,3)	0 (0)	
NYHA				0,665
2	13 (39,4)	8 (42,1)	5 (35,7)	
3	17 (51,5)	10 (52,6)	7 (50,0)	
4	3 (9,1)	1 (5,3)	2 (14,3)	
Etiology				0,348
Primary	4 (12,1)	3 (15,8)	1 (7,1)	
Ventricular	16 (48,5)	8 (42,1)	8 (57,1)	
Atrial	13 (39,4)	8 (42,1)	5 (35,7)	
Daily Furosemide >125 mg/day	3 (9,1)	1 (5,3)	2 (14,3)	0,373
Haemoglobin	116,2 (30,5)	124,3 (23,1)	105,21 (36,4)	0,074
Creatinine	133,0 (81,5)	109,5 (39,3)	164,9 (110,9)	0,052
Albumin	33,6 (4,0)	35,2 (3,2)	30,9 (3,8)	0,003
NT-proBNP	1715,0 [1086,0–4098,75]	1391,0 [893,5–3234,0]	3701 [1689,0–5800]	0,089
sPAP	40.1 ± 11.7	40.8 ± 12.5	39.5 ± 11.4	0,786
Pulmonary Resistance	486.3 ± 445.1	267.9 ± 208.3	677.4 ± 519.2	0,073
TAPSE/sPAP	0,27 [0,19–0,37]	0,23 [0,19–0,38]	0,30 [0,17–0,36]	0,936
TR severity				0,345
Moderate	1 (3,0)	0	1 (7,1)	
Severe	9 (27,3)	4 (21,1)	5 (35,7)	
Massive	13 (39,4)	10 (52,6)	3 (21,4)	
Torrential	10 (30,3)	5 (26,3)	5 (35,7)	
MR				0,886
Mild	21 (63,7)	11 (57,9)	10 (71,4)	
Moderate	9 (27,3)	6 (31,6)	3 (21,4)	
Severe	3 (9,1)	2 (10,5)	1 (7,1)	

Values are median [interquartile range], n (%), or mean ± SD, AF = Atrial Fibrillation, CABG = Coronary Artery Bypass Grafting, CAD = Coronary Artery Disease, CO = Cardiac Output, COI = Cardiac Output Index, HF = heart failure, MI = Myocardial Infarction, MR = Mitral Regurgitation, NYHA = New York Heart Association, PAP = Pulmonary Artery Pressure, PCWP = Pulmonary Capillary Wedge Pressure, PM = Pacemaker, RV = Right Ventricular, RA = Right Atrium, SV = Stroke Volume, TR = Tricuspid Regurgitation.

4.4. Intra- and inter-observer variability test

Apart from echo-derived tenting height, which showed moderate agreement in the interobserver analysis, all CT and echo-derived parameters showed good or excellent intra- and interobserver reliability (Supplemental Table 3).

4.5. Procedural characteristics

T-TEER was performed with the PASCAL device (Edwards Lifesciences, Irvine, CA, USA) in 12 patients (36.4%) and MitraClip or TriClip device (Abbott Laboratories, Abbott Park, IL, USA) in 17 (51.5%). Each patient received a median of two devices [IQR 1–3]. At least one device was implanted in the anteroseptal commissure in 28 cases (84.8%), the posteroseptal commissure in 8 cases (24.2%), and the anteroposterior

commissure in 1 case (3%). In four patients, implantation of the device was not possible due to high risk of single leaflet device attachment related to poor image quality (all four patients) and additionally large coaptation gap (one patient) and posterior jet location (one patient). Concomitant treatment of TR and mitral regurgitation was performed in 18.8% (n = 6) of patients. More than one device was placed in 24 (72.7%) patients. At the end of the procedure, 16 (55.2%), 6 (20.7%), 6 (20.7%) and 1 (3.5%) patients having received a device had mild, moderate, severe and massive TR, respectively (Fig. 3).

4.6. Procedural complexity

The median fluoroscopy time was 14.44 [IQR 12.09–21.16] min. The mean fluoroscopy time needed to implant one device was 9.41 ± 4.86 min and was significantly longer in patients with procedural failure

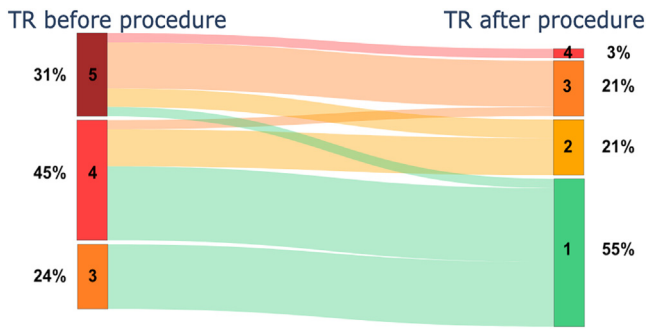


Fig. 3. Diagram showing changes in tricuspid regurgitation severity (1–5) before and after T-TEER.

compared to patients with procedural success (8.05 ± 3.15 vs 12.16 ± 6.6 , $p = 0.036$). The duration of fluoroscopy was not related to the severity of baseline or residual TR (Supplemental Figure 3). Supplemental Table 4 shows the correlations of fluoroscopy times with anatomical parameters. Longer antero-posterior IVC-to-TA distance and IVC-to-TA height, larger RV volumes and length as well as greater TA dimensions correlated significantly with longer fluoroscopy time. Among the previously mentioned parameters, only shorter IVC-to-TA height (ES $r = -0.398$, $p = 0.044$) (Fig. 4) and greater RV length (ES $r = 0.537$, $p = 0.008$, ED $r = 0.551$, $p = 0.006$) correlated with longer fluoroscopy time needed for implantation of one device (Fig. 5A–B).

4.7. Technical success

Technical success was achieved in 26 individuals (79%) and 7

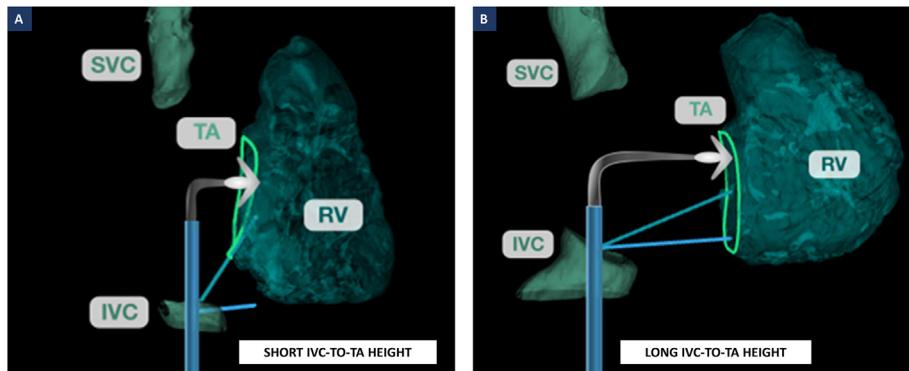


Fig. 4. A shorter IVC-to-TA height hinders the maneuvering and repositioning of the device. Panel A demonstrates anatomy with a short IVC-to-TA height, while panel B shows an anatomy with a longer IVC-to-TA height. In the first case (Panel A), three devices were implanted in the anterosseptal commissure, resulting in a fluoroscopy time of 36 min 40 s (12 min 13 s per device) and TR reduction from torrential to moderate. In the second example (Panel B), two devices were implanted in the anterosseptal commissure with a total fluoroscopy time of 7 min 34 s (3 min 47 s per device), resulting in TR reduction from massive to mild.

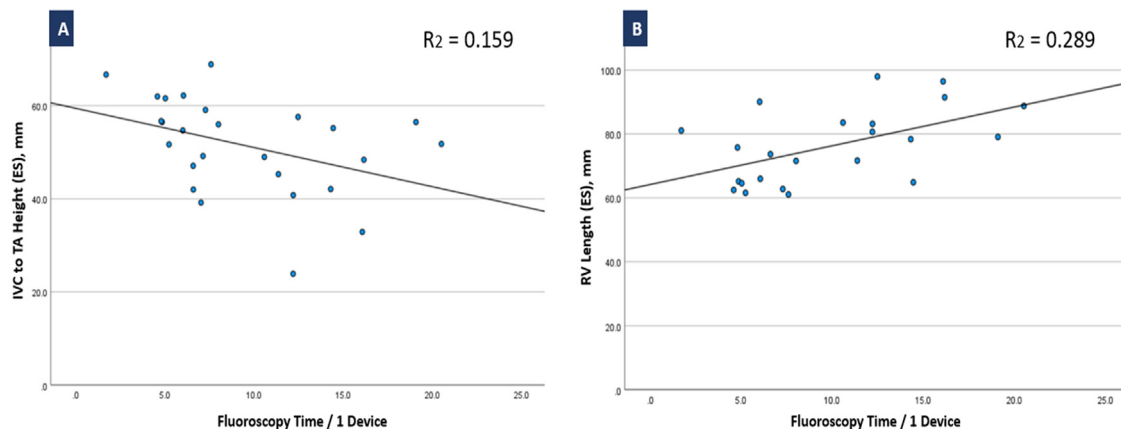


Fig. 5. A. Relationship between IVC-to-TA height and fluoroscopy time for each implanted device. B. Relationship between RV length and fluoroscopy time needed for each implanted device. Grey line is the linear regression line. ES = End-systolic.

patients experienced technical failure. Three patients were diagnosed with single leaflet device attachment. An anatomical comparison revealed that patients with technical failure had greater RV length (ES 88.7 ± 7.8 mm vs 74.6 ± 11.6 mm, $p = 0.009$; ED 94.8 ± 6.2 mm vs 86.0 ± 9.1 mm, $p = 0.037$) and greater IVC-to-TA septo-lateral offset (16.2 ± 10.3 mm vs 8.8 ± 5.6 mm, $p = 0.024$) (Fig. 6). Both of these parameters reduced the probability of successful device implantation in the univariate analysis (OR 0.895 [95% CI 0.809–0.990, $p = 0.031$] and OR 0.866 [95% CI 0.753–0.997, $p = 0.046$] respectively). Greater RV length remained the only anatomical parameter reducing the probability of technical success in the multivariate analysis (adjusted OR 0.812 [95% CI 0.665–0.991], $p = 0.040$; Table 2). Supplemental Table 5 includes a complete list of all parameters tested in the univariate analysis.

Procedural success was achieved in 22 (67% of the overall patient cohort and 76% patients who received a device). In the multivariate analysis, greater RV length emerged as the sole independent predictor significantly associated with a decreased likelihood of procedural success (adjusted OR 0.766 [95% CI 0.591–0.992]; $P = 0.043$); Supplemental Table 6).

4.8. Clinical outcome

The median hospital stay was 3 days [IQR 2–5 days]. Patients were followed for a median of 249 days [IQR 130–563 days]. Throughout the 2-year follow-up period 42% ($n = 14$) of the patients reached the composite endpoint of death, heart failure hospitalization or tricuspid re-intervention. All-cause mortality was observed in 24.2% ($n = 8$) of patients. RV length and RA/RV ratio <2 (indicating secondary TR etiology) were significantly associated with the composite endpoint at two years following the procedure. The association of RV length remained significant after adjustment for age and albumin (adjusted HR 1093 [95% CI

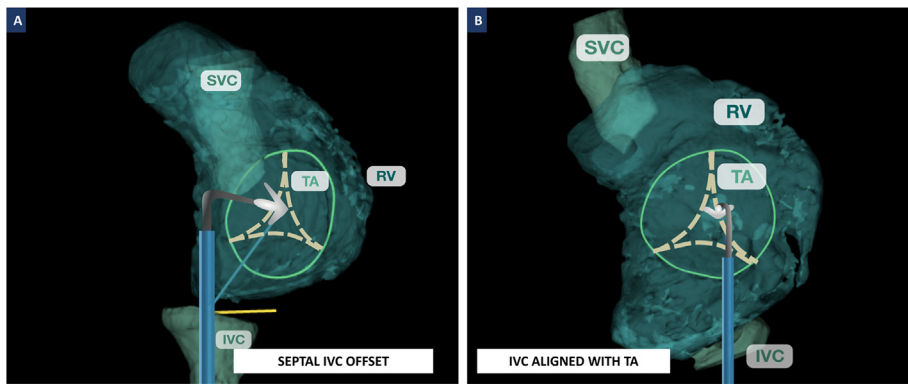


Fig. 6. In the first example (Panel A), the IVC offset is located septal from the middle of the tricuspid annulus. The septal shift of the IVC necessitates rotation of the steering catheter to position the device in the anterosseptal commissure. In such a position, it may be difficult to align the device perpendicular to the valvular plane. The device is often tilted in the commissure, with one arm extending above the anterior leaflet and the other arm below the septal leaflet. In this case, the procedure was terminated because device placement was not feasible. Panel B illustrates an anatomy of the patient whose IVC offset aligns with the center of the TA. This allows a single flex of the steering catheter to position the device perpendicular to the annular plane, facilitating the simultaneous grasping of both leaflets. SVC = Superior Vena Cava.

1004–1191]; $P = 0.040$, Table 3). The risk of experiencing the composite endpoint two years after the index procedure was four-fold higher in “>77.4 mm” group compared to “≤77.4 mm” group, as well as after indexing for body height (“>4.5*10⁻²” group compared to “≤4.5*10⁻²” group; HR = 3.964 [95% CI, 1.018–15.434]; $p = 0,034$, Fig. 7).

4.9. Clinical factors affecting RV length

To put our findings into clinical context, we stratified the cohort according to RV length and compared all baseline clinical, hemodynamic and CT-derived parameters. RV length was greater in patients with pulmonary hypertension (88.5 ± 11.8 vs 73.9 ± 10.2 $p = 0.004$) as well as in patients with V-STR etiology compared to patients with A-STR etiology (81.2 ± 10.8 mm vs 71.4 ± 9.6 mm, $P = 0.027$). Patients with RV length >77.4 mm had lower TAPSE/sPAP values and greater septo-lateral IVC offset, which may be a result of cardiac rotation of the heart along with increasing RV dimensions. Among other CT derived RV, RA and TA parameters RV length correlated strongest with tenting height ($r = 0.849$, $p < 0.001$).

5. Discussion

The major findings of this study are as follows: 1) Greater RV length

Table 2

Univariate and multivariate logistic regression model evaluating predictors of device success.

	Univariate Analysis ^a		Multivariate Analysis	
	Odds ratio [95% CI]	p-value	Odds ratio [95% CI]	p-value
IVC to TA Distance SL ED	0,866 [0,753–0,997]	0,046	0,913 [0,765–1090]	0,316
RV Length ES	0,895 [0,809–0,990]	0,031	0,812 [0,665–0,991]	0,040

ED = End-Diastolic, ES = End-Systolic, IVC = Inferior Vena Cava, RV = Right Ventricle.

^a All automated CT-derived and echocardiographic parameters (see supplemental Table 5) were subjected to analysis. Parameters with a p-value of less than 0.05 in the univariate model, are presented.

Table 3

Univariate and Multivariate Cox Regression Model Evaluating Predictors of the Primary Clinical Outcome (Composite of Death, HF hospitalization or Tricuspid Intervention at Two Years Following the Index Procedure).

	Univariate Analysis		Multivariate Analysis*	
	Hazard ratio (95% CI)	p-value	Hazard ratio (95% CI)	p-value
Age	0,907 (0,847–0,971)	0,005	0,965 (0,853–1091)	0,570
Albumin	0,812 (0,692–0,954)	0,011	0,823 (0,648–1046)	0,111
TAPSE/sPAP	1241 (0,010–149,877)	0,930	–	–
Renal Disease	2374 (0,813–6928)	0,114	–	–
RV Length ES	1095 (1031–1162)	0,003	1093 (1004–1191)	0,040
TAPSE	0,995 (0,840–1,178)	0,951	–	–
RV EF	0,963 (0,919–1,008)	0,107	–	–
PAPi	1,010 (0,957–1,067)	0,706	–	–

EF = Ejection Fraction, ES = End-Systolic, PAPi = pulmonary artery pressure index, RV = Right Ventricle, TAPSE = Tricuspid Annular Plane Systolic Excursion, RV = Right Ventricular, sPAP = systolic pulmonary artery pressure.

and shorter IVC-to-TA height correlate with a longer fluoroscopy time per device and indicate procedural complexity, 2) RV length was the only independent CT anatomical predictor of technical and procedural success 3) shorter RV length was independently associated with lower risk of experiencing the composite endpoint of death, heart failure hospitalization and tricuspid re-intervention at two years.

5.1. Anatomical parameters and fluoroscopy time

Enlargement of the adjacent structures in the absence of a fibrous skeleton leads to tricuspid valve distortion and an increase in the coaptation gap. Larger jets usually require a greater number of devices for substantial TR reduction, which could also explain the observed association between fluoroscopy time of the whole procedure and larger RA, TA and RV dimensions. In contrast, RV length and the IVC-to-TA height were not related to TR severity. This suggests that prolonged fluoroscopy time per device was not solely due to TR severity, but also depended on access to the tricuspid valve and RV size.

5.2. IVC relation to the tricuspid annulus

Several reports have postulated that the anatomical relation of IVC to the TA plays an important role in the procedural outcomes of

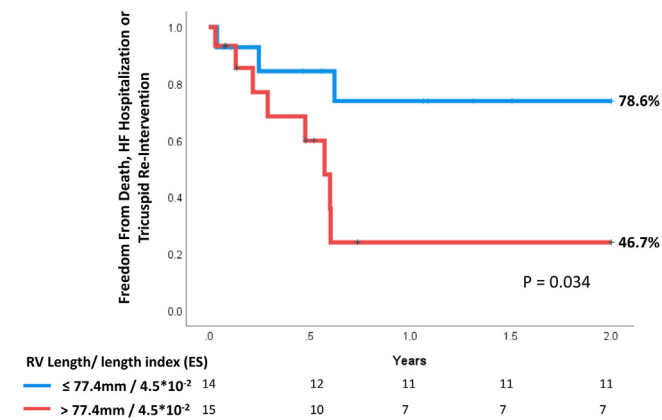


Fig. 7. Kaplan-Meier analysis with log rank test for the combined endpoint (death, heart failure rehospitalization or tricuspid re-intervention) after tricuspid TEER stratified by RV length.

transcatheter valve interventions.^{13,14} The septal or lateral displacement of IVC is generally deemed unfavorable due to the additional rotation of the delivery catheter needed to center the device towards the valve leaflets (Fig. 6). The centration of the device towards the valve from the lateral or medial side tilts the device in the commissural line resulting in one arm of the device being below and another arm above the tricuspid leaflet. This hypothesis provides a potential explanation for the shorter IVC-to-TA septo-lateral offset observed in patients with technical success, in comparison to those without. Whether IVC-to-TA septo-lateral offset increases the probability of single leaflet device attachment may warrant further investigation on a larger sample size.

Furthermore, our analysis showed that a shorter IVC-to-TA height was linked to prolonged fluoroscopy times. In analogy to mitral TEER, where achieving an optimal transseptal puncture height (typically positioned at least 4 cm above the mitral plane) facilitates an appropriate trajectory towards the mitral leaflets for effective grasping,¹⁵ the height between the IVC and TA plays a similar role for tricuspid interventions. In cases with a shorter distance between the IVC and the TA, the available space for maneuvering the device in the RA is restricted, limiting the possibility to make necessary adjustments during the procedure (Fig. 4), which explains the observed prolongation of fluoroscopy time in case of shorter IVC-to-TA height.

5.3. Right ventricular length

Shorter RV length was identified as an independent predictor for technical and procedural success and impacted clinical outcomes. Further analysis showed that RV length correlated strongly with tenting height and was greater in patients with ventricular secondary TR and pulmonary hypertension. Histologically, tricuspid chordae tendineae are composed of straight collagen bundles and less elastic bundles.¹⁶ The less extensible nature of the tricuspid chordae tendineae results in more pronounced tethering of tricuspid leaflets in case of RV dilatation and RV lengthening compared to the mitral valve apparatus.^{16,17} Indeed, Topilsky and colleagues found that RV lengthening and RV sphericity represent the anatomical substrate for tricuspid leaflets tethering.¹⁷ The correlation between greater RV length and leaflet tenting provides a possible explanation for the inferior procedural outcomes observed in patients with longer RVs. Although the bRIGHT study showed a link between RV ED dimension and procedural success,¹⁸ this is the first study to show an association between RV length by CT, and procedural and clinical outcomes with T-TEER.

Several reports have indicated that tenting height is a reliable predictor of recurrent TR after surgical TV repair.^{19–21} However, the available data regarding the impact of tenting on the success of transcatheter interventions are inconsistent.^{1,2,18} The assessment of tenting height and

area by echocardiography can be challenging due to the complexity of tricuspid valve anatomy. Variations in measurement may occur depending on the exact position of the imaging plane, which could explain the conflicting data. Indeed, the echo-derived tenting height showed the weakest interobserver reliability among all manually measured parameters. RV length measured by an automated CT software program could potentially serve as a more reproducible and accurate surrogate of tenting height.

5.4. Clinical outcomes

Patients with the ES RV length >77.4 mm or ES RV length index of $>4.5 \times 10^{-2}$ exhibited a four-fold increase in the risk of experiencing the composite endpoint of death, heart failure hospitalization, and tricuspid valve re-intervention within two years after the index procedure. Patients with RV length >77.4 mm and RV length index $>4.5 \times 10^{-2}$ had more often ventricular secondary TR and pulmonary hypertension, and lower TAPSE/sPAP suggesting more advanced RV damage which could account for the inferior clinical outcomes observed in this patient group. The association between RV length and tenting, along with its predictive value for poorer clinical outcomes, aligns with data from previous studies, where patients with A-STR had better procedural and clinical outcomes compared to patients with V-STR.²²

6. Limitations

Firstly, the modest sample size reduced the statistical power of our analysis so that cautious interpretation of the results is needed and the generalizability may not be possible. Additionally, patients were selected to have adequate renal function to allow for contrast CT. Secondly, CT scans are not typically used for T-TEER screening, however patients referred for transcatheter tricuspid interventions may undergo CT for screening of other tricuspid therapies. Finally, EROA was measured with proximal isovelocity surface area method without correction for flow or tenting angle, which could explain the lack of correlations between the effective regurgitant orifice area and tenting measures. It is noteworthy, that most of the CT-derived parameters were obtained using automated computation only, which helped ensure the reproducibility of the measurements.

7. Conclusion

CT measurements of RV length and anatomical relation between IVC and TA can help identify patients with a higher risk of inferior outcomes following T-TEER and may be useful for preprocedural decision-making and device selection.

Data availability

The data underlying this article will be shared on reasonable request to the corresponding author.

Declaration of competing interest

The authors declare the following financial interests/personal relationships which may be considered as potential competing interests: Dr. Bartkowiak reports research grant from Novartis Foundation. Dr. Windecker reports research, travel or educational grants to the institution without personal remuneration from Abbott, Abiomed, Amgen, Astra Zeneca, Bayer, Braun, Biotronik, Boehringer Ingelheim, Boston Scientific, Bristol Myers Squibb, Cardinal Health, CardioValve, Cordis Medical, Corflow Therapeutics, CSL Behring, Daiichi Sankyo, Edwards Lifesciences, Farapulse Inc. Fummedica, Guerbet, Idorsia, Inari Medical, InfraRedx, Janssen-Cilag, Johnson & Johnson, Medalliance, Medtronic, Merck Sharp & Dohm, Miracor Medical, Novartis, Novo Nordisk, Organon, OrPha Suisse, Pharming Tech. Pfizer, Polares,

Regeneron, Sanofi-Aventis, Servier, Sinomed, Terumo, Vifor, V-Wave. Dr. Windecker served as advisory board member and/or member of the steering/executive group of trials funded by Abbott, Abiomed, Amgen, Astra Zeneca, Bayer, Boston Scientific, Biotronik, Bristol Myers Squibb, Edwards Lifesciences, MedAlliance, Medtronic, Novartis, Polares, Recardio, Sinomed, Terumo, and V-Wave with payments to the institution but no personal payments. He is also member of the steering/executive committee group of several investigator-initiated trials that receive funding by industry without impact on his personal remuneration. Dr. Hahn reports speaker fees from Abbott Structural, Baylis Medical, Edwards Lifesciences, Medtronic and Philips Healthcare; she has institutional consulting contracts for which she receives no direct compensation with Abbott Structural, Edwards Lifesciences, Medtronic and Novartis; she is Chief Scientific Officer for the Echocardiography Core Laboratory at the Cardiovascular Research Foundation for multiple industry-sponsored tricuspid valve trials, for which she receives no direct industry compensation. Dr. Praz has been compensated for travel expenses from Abbott Vascular, Edwards Lifesciences, Polares Medical, Medira, and Siemens Healthineers.

Appendix A. Supplementary data

Supplementary data to this article can be found online at <https://doi.org/10.1016/j.jcct.2024.02.001>.

References

- Besler C, Orban M, Rommel KP, et al. Predictors of procedural and clinical outcomes in patients with symptomatic tricuspid regurgitation undergoing transcatheter edge-to-edge repair. *JACC Cardiovasc Interv.* 2018;11(12):1119–1128.
- Mehr M, Taramasso M, Besler C, et al. 1-Year outcomes after edge-to-edge valve repair for symptomatic tricuspid regurgitation: results from the TriValve registry. *JACC Cardiovasc Interv.* 2019;12(15):1451–1461.
- Sugiura A, Tanaka T, Kavsur R, et al. Leaflet configuration and residual tricuspid regurgitation after transcatheter edge-to-edge tricuspid repair. *JACC Cardiovasc Interv.* 2021;14(20):2260–2270.
- Taramasso M, Alessandrini H, Latib A, et al. Outcomes after current transcatheter tricuspid valve intervention: mid-term results from the international TriValve registry. *JACC Cardiovasc Interv.* 2019;12(2):155–165.
- Khalique OK, Jelmin V, Hueske A, et al. Right heart morphology of candidate patients for transcatheter tricuspid valve interventions. *Cardiovasc Eng Technol.* 2022;13(4): 573–589.
- Hahn RT, Thomas JD, Khalique OK, Cavalcante JL, Praz F, Zoghbi WA. Imaging assessment of tricuspid regurgitation severity. *JACC Cardiovasc Imaging.* 2019;12(3): 469–490.
- Lang RM, Badano LP, Mor-Avi V, et al. Recommendations for cardiac chamber quantification by echocardiography in adults: an update from the American Society of Echocardiography and the European Association of Cardiovascular Imaging. *J Am Soc Echocardiogr.* 2015;28(1):1–39 e14.
- Zoghbi WA, Adams D, Bonow RO, et al. Recommendations for noninvasive evaluation of native valvular regurgitation: a report from the American society of echocardiography developed in collaboration with the society for cardiovascular magnetic resonance. *J Am Soc Echocardiogr.* 2017;30(4):303–371.
- Hahn RT, Badano LP, Bartko PE, et al. Tricuspid regurgitation: recent advances in understanding pathophysiology, severity grading and outcome. *Eur Heart J Cardiovasc Imaging.* 2022;23(7):913–929.
- Hahn RT. State-of-the-Art review of echocardiographic imaging in the evaluation and treatment of functional tricuspid regurgitation. *Circ Cardiovasc Imaging.* 2016;9(12).
- Dreyfus J, Audureau E, Bohbot Y, et al. TRI-SCORE: a new risk score for in-hospital mortality prediction after isolated tricuspid valve surgery. *Eur Heart J.* 2022;43(7): 654–662.
- Hahn RT, Zamorano JL. The need for a new tricuspid regurgitation grading scheme. *Eur Heart J Cardiovasc Imaging.* 2017;18(12):1342–1343.
- Blusztajn DI, Hahn RT. New therapeutic approach for tricuspid regurgitation: transcatheter tricuspid valve replacement or repair. *Front Cardiovasc Med.* 2023;10: 1080101.
- Ranard LS, Vahl TP, Chung CJ, et al. Impact of inferior vena cava entry characteristics on tricuspid annular access during transcatheter interventions. *Cathet Cardiovasc Interv.* 2022;99(4):1268–1276.
- Fan Y, Chan JSK, Lee AP. Advances in procedural echocardiographic imaging in transcatheter edge-to-edge repair for mitral regurgitation. *Front Cardiovasc Med.* 2022;9:864341.
- Lim KO. Mechanical properties and ultrastructure of normal human tricuspid valve chordae tendineae. *Jpn J Physiol.* 1980;30(3):455–464.
- Topilsky Y, Khanna A, Le Tourneau T, et al. Clinical context and mechanism of functional tricuspid regurgitation in patients with and without pulmonary hypertension. *Circ Cardiovasc Imaging.* 2012;5(3):314–323.
- Lurz P, Besler C, Schmitz T, et al. Short-term outcomes of tricuspid edge-to-edge repair in clinical practice. *J Am Coll Cardiol.* 2023;82(4):281–291.
- Kabasawa M, Kohno H, Ishizaka T, et al. Assessment of functional tricuspid regurgitation using 320-detector-row multislice computed tomography: risk factor analysis for recurrent regurgitation after tricuspid annuloplasty. *J Thorac Cardiovasc Surg.* 2014;147(1):312–320.
- Fukuda S, Gillinov AM, McCarthy PM, et al. Determinants of recurrent or residual functional tricuspid regurgitation after tricuspid annuloplasty. *Circulation.* 2006; 114(1 Suppl):I582–I587.
- Min SY, Song JM, Kim JH, et al. Geometric changes after tricuspid annuloplasty and predictors of residual tricuspid regurgitation: a real-time three-dimensional echocardiography study. *Eur Heart J.* 2010;31(23):2871–2880.
- Gavazzoni M, Heilbron F, Badano LP, et al. The atrial secondary tricuspid regurgitation is associated to more favorable outcome than the ventricular phenotype. *Front Cardiovasc Med.* 2022;9:1022755.